Inorganic Chemistry
Article

Inorg. Chem. **2009**, *48*, 11743–11747 **11743**
DOI: 10.1021/ic9017807

Thiacalix[4]arene-Supported Planar Ln_4 (Ln = Tb^{III}, Dy^{III}) Clusters: Toward Luminescent and Magnetic Bifunctional Materials

Yanfeng Bi,[†,‡] Xiu-Teng Wang,[§] Wuping Liao,*[,†] Xinwu Wang,[†] Ruiping Deng,[†] Hongjie Zhang,[†] and Song Gao*[,§]

[†]*State Key Laboratory of Rare Earth Resource Utilization, Changchun Institute of Applied Chemistry, Chinese Academy of Sciences, Changchun 130022, China,* [§]*National Laboratory for Molecular Sciences, State Key Laboratory of Rare Earth Materials Chemistry and Applications, College of Chemistry and Molecular Engineering, Peking University, Beijing 100871, China, and* [‡]*Graduate School of Chinese Academy of Sciences, Beijing 100049, China*

Received September 6, 2009

This paper reports the syntheses, crystal structures, and luminescent and magnetic properties of four tetranuclear Tb^{III} (**1** and **3**) and Dy^{III} (**2** and **4**) complexes supported by *p*-phenylthiacalix[4]arene (H_4PTC4A) and *p*-*tert*-butylthiacalix-[4]arene (H_4TC4A). All four frameworks can be formulated as $[Ln^{III}_4(PTC4A/TC4A)_2(\mu_4\text{-}OH)Cl_3(CH_3OH)_2(H_2O)_3]$, and some methanol and water solvent molecules are occupied in the interstices. The compounds are featured with a sandwichlike unit constructed by two tail-to-tail calixarene molecules and a planar tetragonal $(\mu_4\text{-}OH)Ln_4$ cluster. The photoluminescent analyses suggest that there is an efficient ligand-to-Ln^{III} energy transfer for compounds **1**−**3** and H_4PTC4A is a more efficient "antenna" than H_4TC4A. The Dy^{III} compounds exhibit slow magnetic relaxation behavior of single-molecule magnet nature. The substitution of the *t*-Bu group with a phenyl group at the up-rim of thiacalix[4]arene leads to different extended structures and physical properties of as-synthesized compounds.

Introduction

The molecule-based multifunctional materials are currently stimulating more and more research because of their fundamental qualities[1] and potential applications in optical/nonlinear optical property,[2] porosity,[3] conductivity,[4] and molecular magnets.[5] Among them, the lanthanide-based materials with both magnetism and luminescence have not been studied widely.[6,7] Although lanthanide cations such as Dy^{III} and Tb^{III} have attracted increasing attention in the construction of single-molecule magnets (SMMs) because of their large intrinsic magnetic anisotropy,[8,9] the pure lanthanide SMMs are relatively scarce owing to the difficulty in promoting magnetic interactions between the bridging ligand orbitals and the 4f orbitals of the lanthanide ions. The ligands with orbitals able to overlap the 4f orbitals of the lanthanide

*To whom correspondence should be addressed. E-mail: wpliao@ciac.jl.cn (W.L.), gaosong@pku.edu.cn (S.G.). Tel: +86-431-8526-2036. Fax: +86-431-8569-8041.

(1) (a) Öhrström, L.; Larsson, K. *Molecule-Based Materials*; Elsevier BV: Amsterdam, The Netherlands, 2005. (b) Miller, J. S.; Drillon, M. *Magnetism: Molecules to Materials II*; Wiley-VCH: New York, 2002. (c) Gómez-Romero, P.; Sanchez, C. *Functional Hybrid Materials*; Wiley-VCH: Weinheim, Germany, 2004.

(2) (a) Rikken, G. L. J. A.; Raupach, E. *Nature* **2000**, *405*, 932. (b) Bénard, S.; Leáustic, A.; Pei, Y.; Clément, R. *Chem. Mater.* **2001**, *13*, 159.

(3) (a) Bradshaw, D.; Claridge, J. B.; Cussen, E. J.; Prior, T. J.; Rosseinsky, M. J. *Acc. Chem. Res.* **2005**, *38*, 273. (b) Maspoch, D.; Ruiz-Molina, D.; Veciana, J. *Chem. Soc. Rev.* **2007**, *36*, 770. (c) Harbuzaru, B. V.; Corma, A.; Rey, F.; Atienzar, P.; Jordá, J. L.; García, H.; Ananias, D.; Carlos, L. D.; Rocha, J. *Angew. Chem., Int. Ed.* **2008**, *47*, 1080.

(4) Coronado, E.; Galàn-Mascaros, J. R.; Gomez-Garcia, C. J.; Laukhin, V. *Nature* **2000**, *408*, 447.

(5) (a) Benelli, C.; Gatteschi, D. *Chem. Rev.* **2002**, *102*, 2369. (b) Gatteschi, D.; Sessoli, R. *Angew. Chem., Int. Ed.* **2003**, *42*, 268. (c) Winpenny, R. E. P. *Angew. Chem., Int. Ed.* **2008**, *47*, 7992. (d) Gatteschi, D.; Sessoli, R.; Villain, J. *Molecular Nanomagnets*; Oxford University Press: New York, 2007.

(6) (a) Han, Y. F.; Zhou, X. H.; Zheng, Y. X.; Shen, Z.; Song, Y.; You, X. Z. *CrystEngComm* **2008**, *10*, 1237. (b) Li, Y.; Zheng, F. K.; Liu, X.; Zou, W. Q.; Guo, G. C.; Lu, C. Z.; Huang, J. S. *Inorg. Chem.* **2006**, *45*, 6308. (c) Lescop, C.; Luneau, D.; Rey, P.; Bussière, G.; Reber, C. *Inorg. Chem.* **2002**, *41*, 5566.

(7) (a) Chelebaeva, E.; Larionova, J.; Guari, Y.; Sá Ferreira, R. A.; Carlos, L. D.; Almeida Paz, F. A.; Trifonov, A.; Guérin, C. *Inorg. Chem.* **2008**, *47*, 775. (b) Chelebaeva, E.; Larionova, J.; Guari, Y.; Ferreira, R. A. S.; Carlos, L. D.; Almeida Paz, F. A.; Trifonov, A.; Guérin, C. *Inorg. Chem.* **2009**, *48*, 5983 and references cited therein. (c) Kajiwara, T.; Hasegawa, M.; Ishii, A.; Katagiri, K.; Baatar, M.; Takaishi, S.; Iki, N.; Yamashita, M. *Eur. J. Inorg. Chem.* **2008**, 5565. (d) Li, F. Y.; Xu, L.; Gao, G. G.; Fan, L. H.; Bi, B. *Eur. J. Inorg. Chem.* **2007**, 3405.

(8) (a) Tang, J. K.; Hewitt, I.; Madhu, N. T.; Chastanet, G.; Wernsdorfer, W.; Anson, C. E.; Benelli, C.; Sessoli, R.; Powell, A. K. *Angew. Chem., Int. Ed.* **2006**, *45*, 1729. (b) Chibotaru, L. F.; Ungur, L.; Soncini, A. *Angew. Chem., Int. Ed.* **2008**, *47*, 4126. (c) Hussain, B.; Savard, D.; Burchell, T. J.; Wernsdorfer, W.; Murugesu, M. *Chem. Commun.* **2009**, 1100. (d) Lin, P. H.; Burchell, T. J.; Clérac, R.; Murugesu, M. *Angew. Chem., Int. Ed.* **2008**, *47*, 8848. (e) Gamer, M. T.; Lan, Y. H.; Roesky, P. W.; Powell, A. K.; Clérac, R. *Inorg. Chem.* **2008**, *47*, 6581. (f) Zheng, Y. Z.; Lan, Y. H.; Anson, C. E.; Powell, A. K. *Inorg. Chem.* **2008**, *47*, 10813. (g) Chen, Z.; Zhao, B.; Cheng, P.; Zhao, X. Q.; Shi, W.; Song, Y. *Inorg. Chem.* **2009**, *48*, 3493–3495.

(9) (a) Ishikawa, N.; Sugita, M.; Ishikawa, T.; Koshihara, S.; Kaizu, Y. *J. Am. Chem. Soc.* **2003**, *125*, 8694. (b) Ishikawa, N.; Sugita, M.; Wernsdorfer, W. *J. Am. Chem. Soc.* **2005**, *127*, 3650. (c) Osa, S.; Kido, T.; Matsumoto, N.; Re, N.; Pochaba, A.; Mrozinski, J. *J. Am. Chem. Soc.* **2004**, *126*, 420.

Published on Web 11/23/2009

Scheme 1

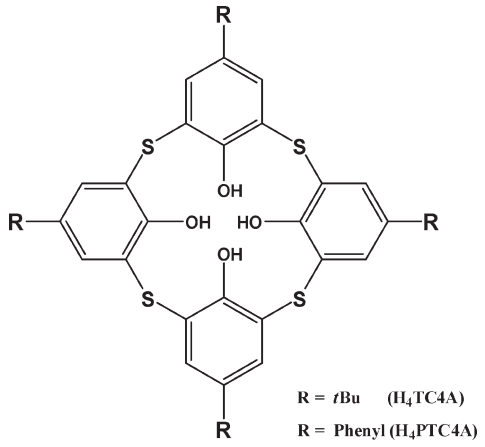

ions should be good candidates for the construction of pure lanthanide-based SMMs. On the other hand, only those ligands that can absorb light in the UV region, transfer the energy via an "antenna effect", and protect the lanthanide ions from vibration coupling which may quench luminescence, are preferred in the construction of luminescent materials.[7c,10] Thus, a well-selected ligand is one of the key factors in building the multifunctional lanthanide-based materials.

p-tert-Butylthiacalix[4]arene (H_4TC4A) and its derivatives (Scheme 1), kinds of multidentate ligands, have been chosen by our group and others to build the metal clusters.[7c,11] Such macrocyclic π-rich ligands [especially the newly synthesized deep-cavity one, *p*-phenylthiacalix[4]arene (H_4PTC4A)] possessing phenoxo groups and sulfur bridges may hold efficient energy-transfer properties for the luminescent materials and the proper orbitals for the construction of lanthanide-based SMMs. Here we present the syntheses, structures, and luminescent and magnetic properties of four Ln^{III}_4 compounds, namely, $[Ln^{III}_4(\mu_4\text{-OH})(PTC4A)_2Cl_3(CH_3OH)_2(H_2O)_3]\cdot m CH_3OH\cdot n H_2O$ (Ln = Tb, m = 4.3, and n = 1.6 for **1**; Ln = Dy, m = 4.7, and n = 2 for **2**) and $[Ln^{III}_4(\mu_4\text{-OH})(TC4A)_2Cl_3(CH_3OH)_2(H_2O)_3]\cdot 9CH_3OH$ (Ln = Tb for **3**; Ln = Dy for **4**).

Experimental Section

Materials and Measurements. *p-tert*-Butylthiacalix[4]arene and *p*-phenylthiacalix[4]arene were synthesized by literature methods,[12,13] and other reagents were purchased from commercial sources and used as received. IR spectra (KBr pellets) were recorded on a Bruker Vertex 70 spectrometer. The element analyses of Tb, Cl, and S were processed on a JEOL JSM-840 scanning electron microscope equipped with an Oxford Link-ISIS-300 energy-dispersive X-ray spectrometer. Fluorescence spectra were obtained on a Hitachi F-4500 fluorescence/phosphorescence spectrophotometer. Magnetic susceptibility measurements for **1**−**4** were performed on a Quantum Design MPMS XL-5 SQUID system in the range of 2−300 K. Diamagnetic corrections for the sample and sample holder were applied to the data.

Syntheses of Compounds 1−4. $[Tb_4(\mu_4\text{-OH})(PTC4A)_2Cl_3(CH_3OH)_2(H_2O)_3]\cdot 4.3CH_3OH\cdot 1.6H_2O$ **(1) and** $[Dy_4(\mu_4\text{-OH})(PTC4A)_2Cl_3(CH_3OH)_2(H_2O)_3]\cdot 4.7CH_3OH\cdot 2H_2O$ **(2).** Colorless crystals of **1**/**2** were obtained from the reaction of a mixture of *p*-phenylthiacalix[4]arene (ca. 0.1 g, 0.125 mmol), $LnCl_3\cdot 6H_2O$ [0.06 g, ca. 0.15 mmol, Ln = Tb (**1**) or Dy (**2**)], $CHCl_3$ (5 mL), CH_3OH (5 mL), and several drops of water in a 20 mL Teflon-lined autoclave that was kept at 130 °C for 3 days and then slowly cooled to 20 °C at about 4 °C h^{-1}. The crystals of **1**/**2** were picked out for X-ray diffraction determination and carefully separated from the mother liquid and washed with CH_3OH and $CHCl_3$ for other measurements. Yield: ∼65% for **1** and 70% for **2** with respect to calixarene, respectively. Energy-dispersive spectrometry analysis of Tb, Cl, and S for **1** reveals a molar ratio of Tb:Cl:S = 4:3.03:8.77, comparable to the expected ratio of 4:3:8 from X-ray diffraction determination.

$[Tb_4(\mu_4\text{-OH})(TC4A)_2Cl_3(CH_3OH)_2(H_2O)_3]\cdot 9CH_3OH$ **(3) and** $[Dy_4(\mu_4\text{-OH})(TC4A)_2Cl_3(CH_3OH)_2(H_2O)_3]\cdot 9CH_3OH$ **(4).** The syntheses of **3** and **4** were similar to those for **1** and **2** except that *p*-phenylthiacalix[4]arene was replaced by *p-tert*-butylthiacalix[4]arene (ca. 0.09 g, 0.125 mmol). However, only a limpid solution was obtained by solvothermal training. Further slow evaporation of the solution afforded compounds **3** and **4**. Yield: ∼40% for **3** and 55% for **4** with respect to calixarene, respectively.

X-ray Crystallographic Analysis. The X-ray intensity data for compounds **1**−**4** were collected on a Bruker APEX-II CCD diffractometer with graphite-monochromatized Mo Kα radiation (λ = 0.710 73 Å) operated at 1.5 kW (50 kV and 30 mA). The crystal structure was solved by means of direct methods and refined employing full-matrix least squares on F^2 (*SHELXTL-97*).[14] All non-hydrogen atoms were refined anisotropically except for the solvent molecules, and hydrogen atoms of the organic ligands were generated theoretically onto the specific atoms and refined isotropically with fixed thermal factors. The disordered Cl2 and O8 sites were refined with an equal occupation factor of 0.5. Hydrogen atoms on coordinated water and methanol molecules and solvent molecules cannot be generated and were included in the molecular formula directly. In addition, the high R1 and wR2 factors of compounds **1**−**4** might be due to the weak high-angle diffractions and disorders. All of the crystal data and structure refinement details for these four compounds are given in Table 1. See the Supporting Information for further details. CCDC numbers 743421−743424 are for **1**−**4**, respectively.

Results and Discussion

Crystal Structures. The essential feature of compounds **1**−**4** were given by the sandwichlike units that result from two tail-to-tail calixarene molecules and an in-between planar tetragonal (μ_4-OH)Ln_4 cluster (Figure 1). Single-crystal X-ray diffraction determination reveals that all four compounds were constructed by some isolated sandwichlike units and the solvent molecules filled in the interstices. On the basis of the structure determination, IR analysis (Figure S1 in the Supporting Information),

(10) (a) Kido, J.; Okamoto, Y. *Chem. Rev.* **2002**, *102*, 2357. (b) Stein, G.; Wurzberg, E. *J. Chem. Phys.* **1975**, *62*, 208.

(11) (a) Kajiwara, T.; Iki, N.; Yamashita, M. *Coord. Chem. Rev.* **2007**, *251*, 1734 and references cited therein. (b) Zeller, J.; Radius, U. *Inorg. Chem.* **2006**, *45*, 9487. (c) Desroches, C.; Pilet, G.; Borshch, S. A.; Parola, S.; Luneau, D. *Inorg. Chem.* **2005**, *44*, 9112. (d) Bilyk, A.; Hall, A. K.; Harrowfield, J. M.; Hosseini, M. W.; Skelton, B. W.; White, A. H. *Aust. J. Chem.* **2000**, *53*, 895. (e) Bi, Y. F.; Li, Y. L.; Liao, W. P.; Zhang, H. J.; Li, D. Q. *Inorg. Chem.* **2008**, *47*, 9733. (f) Bi, Y. F.; Wang, X. T.; Wang, B. W.; Liao, W. P.; Wang, X. F.; Zhang, H. J.; Gao, S.; Li, D. Q. *Dalton Trans.* **2009**, 2250. (g) Kajiwara, T.; Katagiri, K.; Hasegawa, M.; Ishii, A.; Ferbinteanu, M.; Takaishi, S.; Ito, T.; Yamashita, M.; Iki, N. *Inorg. Chem.* **2006**, *45*, 4880. (h) Bi, Y. F.; Wang, X. T.; Liao, W. P.; Wang, X. F.; Wang, X. W.; Zhang, H. J.; Gao, S. *J. Am. Chem. Soc.* **2009**, *131*, 11650. (i) Bi, Y. F.; Liao, W. P.; Wang, X. W.; Deng, R. P.; Zhang, H. J. *Eur. J. Inorg. Chem.* **2009**, 4989.

(12) Lhoták, P.; Šmejkal, T.; Stibor, I.; Havlíček, J.; Tkadlecovč, M.; Petříčková, H. *Tetrahedron Lett.* **2003**, *44*, 8093.

(13) Iki, N.; Kabuto, C.; Fukushima, T.; Kumagai, H.; Takeya, H.; Miyanari, S.; Miyashi, T.; Miyano, S. *Tetrahedron.* **2000**, *56*, 1437.

(14) Sheldrick, G. M. *Acta Crystallogr., Sect. A: Found. Crystallogr.* **2008**, *64*, 112.

Table 1. Crystal Data and Structure Refinement for Compounds **1**−**4**

	1	**2**	**3**	**4**
formula	$C_{102.32}H_{91.44}Cl_3Tb_4O_{19.90}S_8$	$C_{102.65}H_{93.64}Cl_3Dy_4O_{20.66}S_8$	$C_{91}H_{139}Cl_3Tb_4O_{23}S_8$	$C_{91}H_{139}Cl_3\ Dy_4O_{23}S_8$
fw	2637.86	2670.61	2599.53	2613.85
cryst syst	monoclinic	monoclinic	triclinic	triclinic
space group	$P2_1/c$	$P2_1/c$	$P\bar{1}$	$P\bar{1}$
a (Å)	15.6478(7)	15.6309(6)	12.3042(5)	12.2728(10)
b (Å)	12.0168(6)	11.9638(4)	15.4867(6)	15.4561(14)
c (Å)	32.3809(12)	32.2831(10)	15.6801(7)	15.6682(14)
α (deg)	90	90	70.6520(10)	70.7390(10)
β (deg)	118.741(2)	118.568(2)	72.5140(10)	72.5420(10)
γ (deg)	90	90	81.7520(10)	81.8020(10)
V (Å^3)	5338.7(4)	5302.1(3)	2685.65(19)	2673.4(4)
Z	2	2	1	1
D_c/g cm^{-3}	1.641	1.673	1.607	1.624
μ/mm^{-1}	2.913	3.086	2.896	3.059
F(000)	2607	2636	1308	1312
total no. of data	28 677	31 323	14 364	18 737
no. of unique data	9375	9335	9390	9336
R_{int}	0.029	0.032	0.019	0.027
GOF	1.067	1.098	1.052	1.106
R1[a] [$I > 2\sigma(I)$]	0.0528	0.0520	0.0350	0.0371
wR2[b] (all data)	0.1533	0.1642	0.0966	0.1091

[a] $R1 = \sum||F_o| - |F_c||/\sum|F_o|$. [b] $wR2 = \{\sum[w(F_o^2 - F_c^2)^2]/\sum[w(F_o^2)^2]\}^{1/2}$.

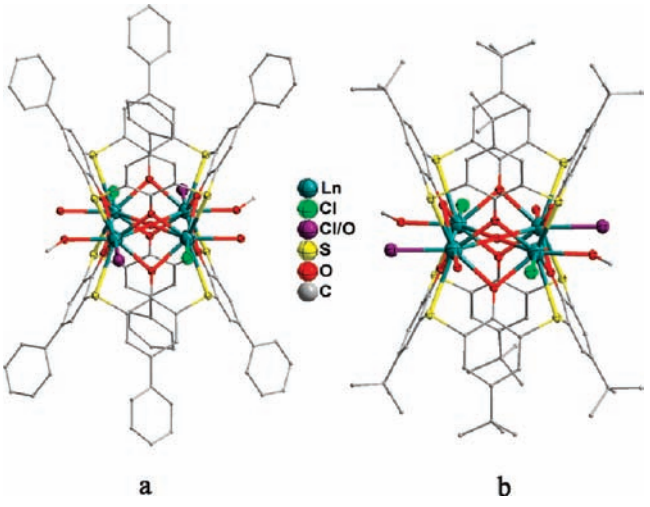

Figure 1. Molecular structures of compounds **1**/**2** (a) and **3**/**4** (b). The hydrogen atoms and isolated solvent molecules are omitted for clarity.

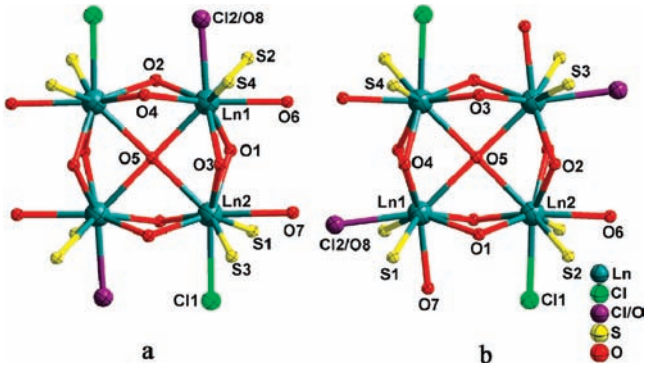

Figure 2. Coordination environment of the metals in compounds **1**/**2** (a) and **3**/**4** (b).

and charge-balance considerations, we found that the basic formula of these four structures should be $[Ln^{III}_4(\mu_4\text{-OH})(PTC4A/TC4A)_2Cl_3(CH_3OH)_2(H_2O)_3]$. Compounds **1** and **2**, or **3** and **4**, are isomorphous and showed similarity in the coordination environment except the slight differences in the bond lengths and angles, respectively (Table S1 in the Supporting Information). Here only the structures of **1** and **3** are described as the examples as below.

There are two crystallographic sites for the metal atoms (Ln1 and Ln2), adopting a Ln1−Ln2−Ln1A−Ln2A quadrilateral mode in all the four cases, as shown in Figure 2. Both Ln1 and Ln2 are nine-coordinated by four phenoxo oxygen atoms, two sulfur atoms, a μ_4-OH, and two other components (i.e., water oxygen, methanol oxygen, and/or chloride anions). It should be noted that the Ln1−Cl2/O8 distance (i.e., 2.62 Å in **1** and 2.70 Å in **3**) is shorter than the bond distance of Ln2−Cl1 (i.e., 2.80 Å in **1** and **3**) because of the site share of Cl2 and O8. Ln1, Ln2, and two metal sites generated by the symmetry operation are bridged by eight phenoxo oxygen atoms and a μ_4-OH, with Ln1−Ln2−Ln1A and Ln2−Ln1−Ln2A angles being 89.42° and 90.58° for **1** and 89.64° and 90.36° for **3**, respectively. The Ln−Ln distances in the edge (linked by $O_{phenoxo}$) and the cross (linked by μ_4-OH) of the Ln^{III}_4 square are 3.56−3.60 and 5.02−5.08 Å for **1** and **3**, respectively. The Ln−$O_{phenoxo}$−Ln angles are in the range of 97.8−98.5° in **1** and 97.9−99.2° in **3**, which are similar to those in the Dy^{III}_3 core bridged by a μ-phenoxo ligand with SMM properties.[8a] Furthermore, the Ln^{III}_4 square is bonded by two tail-to-tail thiacalix[4]arene ligands to form a sandwichlike entity. In a sandwichlike unit, two planes formed by the bridging sulfur atoms from the upper and bottom calixarenes are parallel to each other, which differs from the cases in the heterometallic $Mn_2Gd_2(TC4A)_2$ sandwich (with the dihedral angle being ca. 14°)[11e] and [Mn_2Gd_4(or Mn_2Eu_4)-(*p*-*tert*-butylsulfinylcalix[4]arene)$_4$] double dumbbell (with the dihedral angle being ca. 7°).[11f]

Although all of the tetranuclear sandwichlike units exhibit similar coordination environments and geometries, their stacking differs greatly in the four cases. In compounds **1** and **2**, one phenyl group from one sandwichlike unit protrudes into the cavity of an opposite

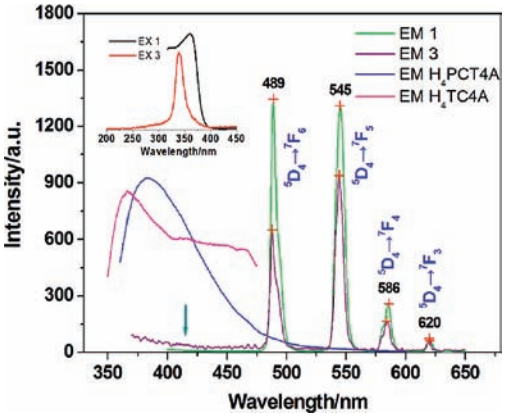

Figure 3. Photoluminescent spectra of **1**, **3**, H_4PTC4A, and H_4TC4A in the solid state at room temperature. Luminescence of the ligand was observed for complex **3** (indicated with an arrow). Inset: Excitation spectra of **1** and **3**.

PTC4A from another sandwich and vice versa to form a dimeric "hand-shake" motif[15] (Figure S2 in the Supporting Information), with the C−H···π interactions being of ca. 3.48 and 3.54 Å. Then all of the tetranuclear units are interconnected head-to-tail with each other to form some chains. Differently, in compounds **3** and **4**, the "parallel" tetranuclear units are interconnected by C−H···O/C−H···Cl interactions (being 2.65−2.91/2.91−3.24 Å) between the isolated methanol and coordinated water molecules/chloride anions to form some shoulder-to-shoulder arrays, and then these parallel 1D arrays are stacked into a 3D extended structure. The different package of the tetranuclear units leads to the different extended structures (Figure S3 in the Supporting Information). The nearest Ln···Ln distance between two adjacent sandwichlike units is ca. 7.34 Å in **1** and **2**, which is shorter than that in **3** and **4** (ca. 7.61 Å). That is, the substitution of the *t*-Bu group with a *p*-phenyl group at the up-rim of thiacalix[4]arene influences the packing mode of the as-synthesized compounds. In view of the attracting progress achieved for H_4TC4A and its derivatives,[11] especially in the cluster chemistry, the H_4PTC4A ligand would be another promising multidentate candidate for construction of the polynuclear compounds.

Luminescent Properties. The solid-state luminescences of compounds **1**−**4** were investigated at room temperature (Figures 3 and 4). Upon excitation at 360/338 nm, compounds **1** and **3** show a green luminescence and the obtained emission spectra can be ascribed to the characteristic f → f transitions [620, 586, 545, and 489 nm, $^5D_4 \rightarrow {}^7F_J$ (J = 3−6)]. This means that the TC4A and PTC4A ligands process efficient energy transfer to the Tb^{III} ion. It is noted that the PTC4A ligand, which prevents back-transfer processes from Tb^{III}, should be a more efficient "antenna" than TC4A because ligand fluorescence is observed in **3** but completely vanishes in **1**. As reported,[11g] the slight difference in the ligand-based S_1 and T_1 levels may lead to significant differences in the luminescent properties, and therefore the match of the energy of the ligand T_1 state and the excited Tb^{III}* state is a key factor for the luminescent properties of the compounds. As shown in Figure 3, the emission peak at 489 nm becomes dominant in **1**, which differs much from the common emissions of Tb^{III}-based materials (commonly, the strongest emission is located at ca. 545 nm, which is assigned to the $^5D_4 \rightarrow {}^7F_5$ transition). The emissions of compound **3** are monitored by Tb^{3+} $^5D_4 \rightarrow {}^7F_5$ at 545 nm, which exhibits a common luminescent property of Tb^{III} compounds.

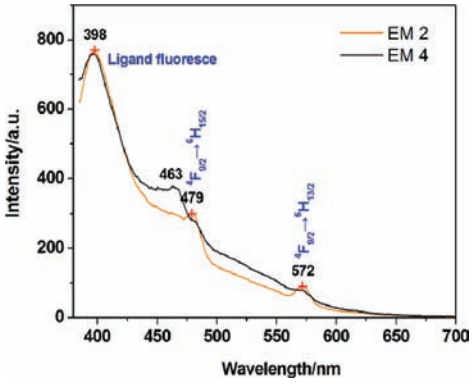

Figure 4. Emission spectra of **2** and **4** in the solid state at room temperature.

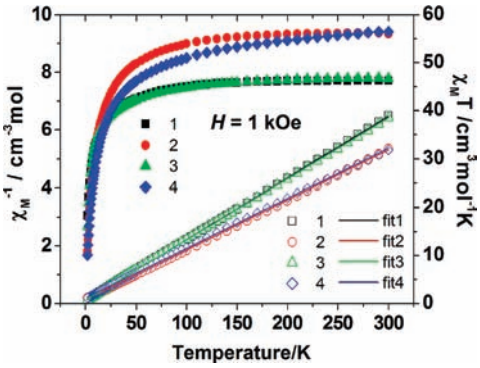

Figure 5. Plots of $\chi_M T$ vs T and $1/\chi_M$ vs T for **1**−**4** in a 1 kOe field. Lines represent Curie−Weiss fittings.

Ligand-based luminescence was observed at ca. 398 nm for both compounds 2 and 4. Photoluminescences were recorded in the range of 385−700 nm under excitation at 365 nm, as shown in Figure 4. There are three main peaks at 398, 479, and 572 nm in the emission spectra of **2**, while there are only two emission peaks at 398 and 463 nm for **4**. The strongest emission band for both compounds is located at ca. 398 nm, which can be assigned to ligand fluorescence because PTC4A and TC4A show broad emissions in the region of 350−525 nm. The emission peaks at 479 and 572 nm for **2** can be assigned to the $^4F_{9/2} \rightarrow {}^6H_{15/2}$ and $^4F_{9/2} \rightarrow {}^6H_{13/2}$ transitions of Dy^{3+}, respectively. The shoulder peak at ca. 463 nm for **4** can also be assigned to ligand fluorescence.

Magnetic Properties. Magnetic studies were performed on the polycrystalline samples of **1**−**4**. At room temperature (300 K), the $\chi_M T$ values are 46.24 and 46.69 cm^3 K mol^{-1} for **1** and **3** (Figure 5), respectively, which are close to the expected value of 47.28 cm^3 K mol^{-1} for four independent Tb^{III}_4 ions (J = 6, S = 3, g = $^3/_2$, $^7F_6$).[9c] The $\chi_M T$ values are almost constant over the whole temperature range except for a decrease in the lower temperature

(15) Carruthers, C.; Ronson, T. K.; Sumby, C. J.; Westcott, A.; Harding, L. P.; Prior, T. J.; Rizkallah, P.; Hardie, M. J. *Chem.—Eur. J.* **2008**, *14*, 10286.

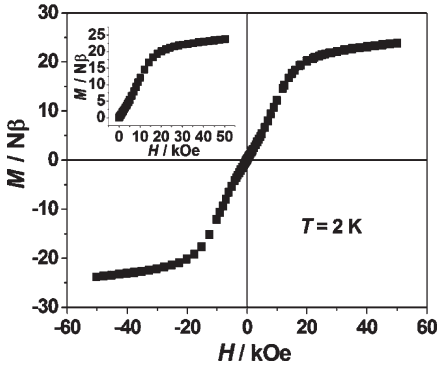

Figure 6. Field dependence of the magnetization of **2** at 2 K. Inset: $M-H$ plot at 2 K.

region. For **2** and **4**, the observed $\chi_M T$ values at room temperature are 56.04 and 56.44 cm^3 K mol^{-1}, which are consistent with the calculated value 56.68 cm^3 K mol^{-1} of four Dy^{III} ions ($J = {}^{15}/_2$, $S = {}^{5}/_2$, $g = {}^{4}/_3$, ${}^6H_{15/2}$).[8] Upon cooling, the $\chi_M T$ value gradually decreases for **4**, whereas the value remains roughly constant before 100 K for **2**. Below 100 K, the $\chi_M T$ values decrease dramatically to 10.96 and 10.13 cm^3 K mol^{-1} at 2 K for **2** and **4**, respectively. The slight different magnetic behaviors observed for **1** and **3** or **2** and **4** might be due to the different stacking of the tetranuclear units, which leads to different ligand fields and further influences the Ln^{III} nature.[8b,f]

Fitting the experimental data ranging from 2 to 300 K to Curie−Weiss law gives Curie constants (C) of 46.96, 57.51, 47.53, and 58.52 cm^3 mol^{-1} K and Weiss constants (θ) of −4.66, −7.86, −5.38, and −11.04 K for **1**−**4**, respectively. The negative Weiss constant (θ) suggests some antiferromagnetic interactions between spin carriers. For the M vs H plot (Figures 6 and S4 in the Supporting Information), the maximum values for M are 23.81 μ_B (for **2**) and 21.95 μ_B (for **4**) at 5 T, which are slightly larger than the calculated value for four uncorrelated Dy^{III} magnetic moments (4×5.23 μ_B)[8a] but close to the values reported by Powell and Clérac's groups.[8d−f] The miss of saturation on the M vs H data at 2 K for Dy^{III} compounds suggests the presence of significant anisotropy and/or low-lying excited states, in agreement with the $\chi_M T$ vs T data and the small Weiss constants.[8e,f] In addition, it is noted that the M vs H plots for **2** and **4** do not show hysteresis above 2 K.

Alternating-current (ac) susceptibility measurements were made to further reveal the magnetic properties of these four compounds. For the two Dy^{III} compounds, compound **2** was depicted in detail as an example because of the similar coordination environments of **2** and **4**. The ac susceptibilities of **2** show obvious frequency-dependent behavior at the zero field ranging from 2 to 20 K (Figure S5 in the Supporting Information), indicating the possible SMM behavior. Moreover, under an intermediate direct-current (dc) field (1 kOe, 2−16 K;Figure 7), the obvious out-of-phase ac signals indicate a slow relaxation of magnetization. The introduction of a dc field might enhance the gap of magnetic energy levels of compound **2**, which leads to an unusual field-dependent magnetic relaxation

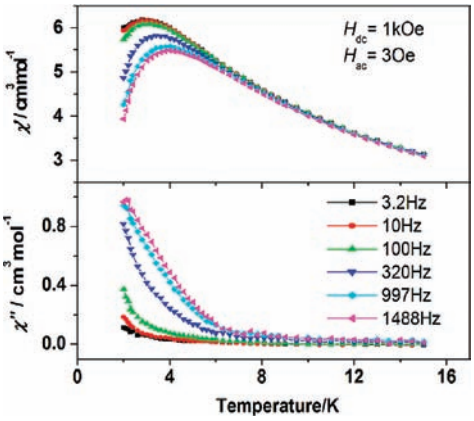

Figure 7. Temperature dependence of the in-phase (top) and out-of-phase (bottom) components of the ac magnetic susceptibility for **2** in a static applied dc field of 1 kOe and an ac field of 3 Oe.

behavior.[8e−g] A similar phenomenon was observed by Gao's group and other groups.[7d,16] Because the slow relaxation of magnetization is experimentally observed only over a short range of temperature and frequency, the estimation of characteristic parameters of τ_0 and U_{eff} was not successful using Arrhenius law. For the Tb^{III} compounds, neither obvious peaks of ac susceptibility nor frequency dependencies were observed (Figure S6 in the Supporting Information; **1** was measured as an example), which indicated no SMM behavior above 2 K.

Conclusions

In summary, four lanthanide-based (Ln = Tb^{III}, Dy^{III}) tetranuclear clusters supported by thiacalix[4]arene (PTC4A and TC4A) are successfully synthesized and structurally characterized, respectively. Structural analyses reveal that compounds **1**−**4** are stacked by some sandwichlike units constructed by two tail-to-tail calixarene molecules and an in-between planar tetragonal (μ_4-OH)Ln_4 cluster. Ligand-to-Ln^{III} energy transfer is effectual for compounds **1**−**3**. Interestingly, the replacement of the *t*-Bu group by a *p*-phenyl group at the up-rim of thiacalix[4]arene leads to different extended structures and a kind of multifunctional material with photoluminescence and SMM-like properties such as compound **2**. The extension of this study to the whole lanthanide series and/or transition metals might shed light on the design and syntheses of the new molecule-based multifunctional materials.

Acknowledgment. This work was supported by the National Natural Science Foundation of China (Grants 50704029 and 20971119), the S&T Development Program of Jilin Province (Grant 20080116), and the project sponsored by SRF for ROCS, Ministry of Education of China.

Supporting Information Available: Crystallographic data in CIF format, IR spectra, additional figures, and other materials. This material is available free of charge via the Internet at http://pubs.acs.org.

(16) (a) Gao, S.; Su, G.; Yi, T.; Ma, B. Q. *Phys. Rev. B* **2001**, *63*, 054431. (b) Ma, B. Q.; Gao, S.; Su, G.; Xu, G. X. *Angew. Chem., Int. Ed.* **2001**, *40*, 434. (c) Zhang, Y. Z.; Duan, G. P.; Sato, O.; Gao, S. *J. Mater. Chem.* **2006**, 2625. (d) Wang, X.-T.; Wang, B.-W.; Wang, Z.-M.; Gao, S. *Inorg. Chim. Acta* **2008**, *361*, 3895.